ARTICLE

Three Dimensional Quantitative Structure Activity Relationship and Molecular Docking Studies of Flavonoids as Reverse Transcriptase Inhibitors

Bikash Kumar Sarkar[1] and Nabanita Giri[2,✉]

Asian Pub. Corp.

www.asianpubs.org

Asian Journal of Organic & Medicinal Chemistry

Volume: 6 Year: 2021
Issue: 1 Month: January–March
pp: 33–39
DOI: https://doi.org/10.14233/ajomc.2021.AJOMC-P303

Received: 15 December 2020
Accepted: 10 February 2021
Published: 24 March 2021

ABSTRACT

A set of 29 flavonoid molecules are used to generate comparative molecular field analysis (CoMFA) and comparative molecular similarity indices analysis (CoMSIA) models. The best CoMFA model showed a cross-validated correlation coefficient (q^2) = 0.762, non-cross-validated correlation coefficient (r^2) = 0.939, standard error of estimate (S) = 0.038 and F = 396. And that for CoMSIA model were q^2 = 0.758, r^2 = 0.957, S = 0.063 and F = 236. The models show a high predictive ability, validated by 11 favonoid molecules. The docking studies shows the hydrogen bonding interaction is mostly responsible for binding of the flavonoids molecules in the binding pocket of HIV 1-RT protein (3HVT.pdb).

KEYWORDS

AMV-RT, Flavonoids, CoMFA, CoMSIA, Docking.

INTRODUCTION

Reverse transcriptase (RT), a multifunctional enzyme, shows biochemical activities namely RNA-dependent and DNA-dependent DNA polymerases and ribonuclease H activities [1,2]. Since reverse transcriptase from HIV-1 is one of the target enzymes for best known anti-AIDS drugs, it has immense medical attentiveness. The avian myeloblastosis virus (AMV) is generally a type C oncogenic RNA virus and related with lymphomas and leukemia [3]. It is well studied that an RNA-dependent DNA polymerase-RT is present in AMV and hence, the investigation of AMV-RT inhibitor as an important anti-tumor agent attracted interests. HIV-1 RT as well as AMV-RT is, basically, hetero-dimers consisting of two different monomer subunits [3,4]. Azidothymidine (AZT), an example of nucleoside HIV-1 RT inhibitor used as an approved drug for HIV infection, also shows encouraging activity of AMV-RT inhibition [5]. AMV-RT inhibitors, hence, may play an important role in the development of potent anti-HIV drugs. Flavonoids are essentially secondary metabolites and show several biological and pharmacological activities with little toxicity [6]. Different biological items like foods, flowers, plants, *etc*. are the natural sources of flavonoids. Various biological activities of flavonoids as antioxidant, anti-inflammatory, antimicrobial, anti-allergic, estrogenic and anti-HIV activities have been studied [7-9]. Some natural flavo-

Author affiliations:

[1]Department of Physics, Mrinalini Datta Mahavidyapith, Birati, Kolkata-700051, India
[2]Department of Microbiology, Acharya Prafulla Chandra College, Kolkata-700 131, India

✉To whom correspondence to be addressed:

E-mail: nabanita_micro@yahoo.com

Available online at: http://ajomc.asianpubs.org

noids are capable to inhibit different types of reverse transcriptase from different sources [10]. Some naturally occurring flavonoids exhibit inhibitory activities against AMV-RT [11]. To acquire the flavonoids' structure-activity relationship (SAR) as a potential RT inhibitor, three-dimensional quantitative structure-activity relationship (3D-QSAR) methods were used. These methods were comparative molecular field analysis (CoMFA) and comparative molecular similarity index analysis (CoMSIA). The most commonly employed CoMFA is based on the concept that interactions between receptors and their ligands mainly have non-covalent nature and are shape independent. Therefore, a QSAR may be acquired by sampling electrostatic (Coulombic) and steric (Lennard-Jones) fields surrounding a ligand set and by correlating differences observed in these fields to the biological activity. To derive the optimum possible QSAR equation, the partial least squares (PLS) analysis together with the cross-validation method was employed for selecting fitting components from a substantial set of CoMFA data [12,13].

The CoMSIA method is the modified version of CoMFA. The steric, hydrophobic, electrostatic and hydrogen bonding properties are included in this method and it is less alignment-dependent than CoMFA [14,15]. Property fields based on similarity indices of molecules aligned commonly are computed through CoMSIA approach. Gaussian-type distance dependence potentials are employed in CoMSIA fields. The exponential dependence from distance keeps away from the occurrence of singularities at the atomic positions. Partial least squares (PLS) analysis is used to compute the fields. Furthermore, docking simulation was executed with some selected flavonoids to verify whether these flavonoids can show activity against HIV 1-RT or not.

EXPERIMENTAL

Biological data: Twenty-nine flavonoids with an AMV-RT inhibition activity were acquired from literature [11] (Table-1). The inhibition activity, that is, the concentration for the 50% of inhibition (IC_{50}), was converted into log (IC_{50}) and

TABLE-1
MOLECULAR STRUCTURES OF FLAVONOID MOLECULES AND THEIR RADICAL SCAVENGING ACTIVITIES IN LOGARITHM SCALE

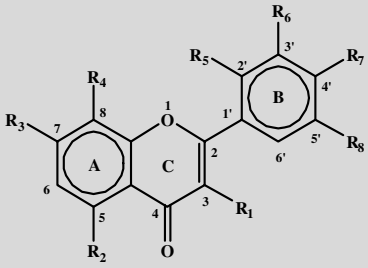

(1-23)

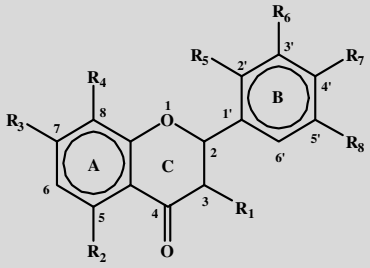

(24-29)

No	Name	R_1	R_2	R_3	R_4	R_5	R_6	R_7	R_8	IC_{50}	pIC_{50}
1	Kaempferol	OH	OH	OH	H	H	H	OH	H	8.5	0.929
2#	Galangin	OH	OH	OH	H	H	H	H	H	9.8	0.991
3	Quercetin	OH	OH	OH	H	H	OH	OH	H	12.2	1.086
4	Kaempferol 3,7-dirh	Orh	OH	Orh	H	H	H	OH	H	15.4	1.188
5#	Robinetin	OH	H	OH	H	H	OH	OH	OH	17.6	1.246
6	Fisetin	OH	H	OH	H	H	OH	OH	H	19.0	1.279
7	3-hydroxyflavone	OH	H	H	H	H	H	H	H	21.3	1.328
8#	Laricytrin	OH	OH	OH	H	H	OH	OH	OMe	22.0	1.342
9	Laricytrin 3'-O-glucoside	OH	OH	OH	H	H	Ogl	OH	OMe	23.3	1.367
10	Myricetin	OH	OH	OH	H	H	OH	OH	OH	23.6	1.373
11	3,5,7,3',4',5' Hexameth. flavones	OMe	OMe	OMe	H	H	OMe	OMe	OMe	28.0	1.447
12	Quercetin 3-O-glu-7-O-rha	Ogl	OH	Orh	H	H	OH	OH	H	31.3	1.496
13#	Rutin	Oru	OH	OH	H	H	OH	OH	H	32.7	1.515
14	Morin	OH	OH	OH	H	OH	H	OH	H	34.9	1.543
15	Flavone	H	H	H	H	H	H	H	H	36.9	1.567
16	5-Hydroxyflavone	H	OH	H	H	H	H	H	H	40.5	1.607
17#	7-Hydroxyflavone	H	H	OH	H	H	H	H	H	45.6	1.659
18	Crysin	H	OH	OH	H	H	H	H	H	48.0	1.681
19	8-Methoxyflavone	H	H	OMe	H	H	H	H	H	50.9	1.707
20	Apigenin	H	OH	OH	H	H	H	OH	H	52.7	1.722
21	Vitexin	H	OH	OH	Gl	H	H	OH	H	59.7	1.776
22	Apigenin 7-O-glucoside	H	OH	Ogl	H	H	H	OH	H	64.6	1.810
23	Luteolin 7-O-glucoside	H	OH	Ogl	H	H	OH	OH	H	68.1	1.833
24	Flavanone	H	H	H	H	H	H	H	H	71.4	1.854
25	Naringenin	H	OH	OH	H	H	H	OH	H	72.6	1.861
26	Naringin	H	OH	One	H	H	H	OH	H	82.5	1.919
27	Hesperetin	H	OH	OH	H	H	OH	OMe	H	85.1	1.930
28	Fustin	OH	H	OH	H	H	OH	OH	H	87.5	1.942
29	Taxifolin (dih)	OH	OH	OH	H	H	OH	OH	H	87.5	1.945

test set of molecules

was abbreviated as pIC_{50}. The overall dataset was divided into training (23 molecules) and testing (5 molecules) sets. The training and testing set were used to produce a QSAR model and to measure external predictivity, respectively.

For the establishment of 3D CoMSIA and CoMFA QSAR models and all the calculations, Sybyl X molecular modeling package [16] was employed. The structural energy of all the 29 molecules was minimized using the Tripos force field by employing the Powell gradient algorithm having a convergence criterion of 0.001 kcal mol^{-1}. The Gasteiger-Hückel method was used to calculate the partial atomic charges.

Molecular alignment: Molecular alignment is an important step in the CoMFA and CoMSIA models development [17]. In this process, the first step is selecting a template molecule to be the molecule 29 exhibiting the highest anti-HIV activity. Into a lattice box, the flavonoid molecules were aligned by fitting with a common portion (napthoquinone moiety) of all the molecules on the template molecule 29. Fig. 1 illustrates the aligned molecule sets.

CoMFA and CoMSIA setup: The CoMFA and CoMSIA models play an important role in the investigation of quantitative correlation between molecular structures and its response properties. Separate CoMFA and CoMSIA models were built for the data set of aligned molecules. By constructing a 3D cubic lattice of grid spacing with 1 Å extending up to 4 Å units beyond the aligned molecules in *x*, *y* and *z* directions, the CoMFA and CoMSIA descriptor fields were derived. Tripos force field was utilized to calculate the Van dar Waals and Coulombic potentials.

In the CoMFA approach, an sp^3-hybridized carbon atom having a +1 charge was employed as a probe atom to produce electrostatic and steric fields. Initially, for both electrostatic and steric energies, a cut off value of 30 kcal/mol was selected.

The CoMSIA approach was acquired using the lattice box employed for the CoMFA method. In the CoMSIA approach, five physico-chemical properties were evaluated. These properties were electrostatic, steric, hydrophobic, hydrogen bond acceptor and hydrogen bond donor. For this evaluation, a common probe atom having a 1 Å radius, +1 hydrophobicity, +1 charge and both hydrogen bond properties +1 was used. To calculate the similarity indices, dependence of the Gaussian type distance was employed between the probe and atoms of the aligned molecules. The default attenuation factor value was set at 0.3.

Model derivation and validation: The partial least squares (PLS) analysis was used to construct the 3D QSAR models. This analysis is an extension of the multiple regression analysis, where CoMSIA and CoMFA fields and pIC_{50} values were treated as independent and dependent variables, respectively. For cross-validation, the leave-one-out (LOO) method, where one mole-

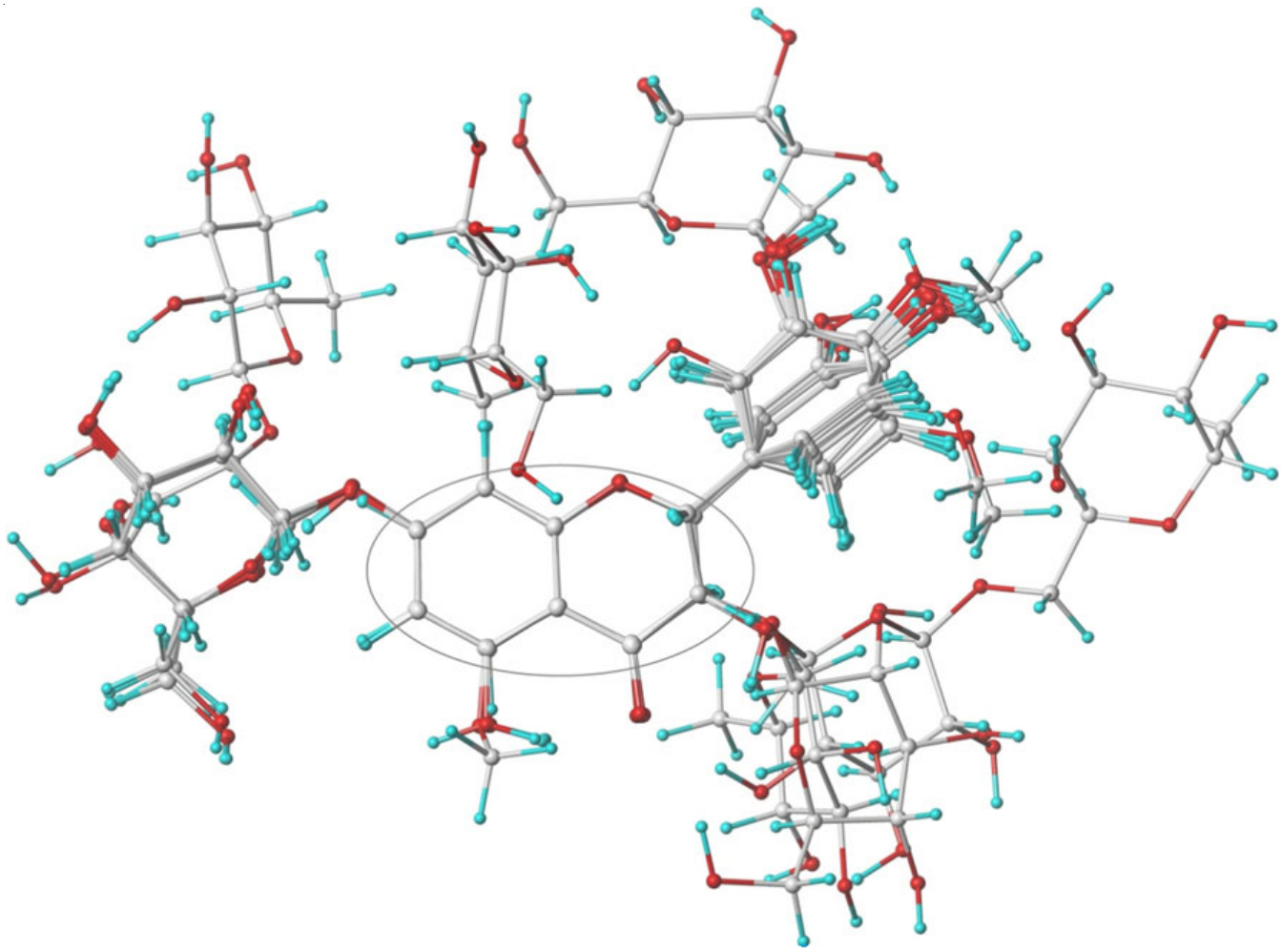

Fig. 1. Molecules have been aligned over the template molecule 29. The common moiety is one of the phenyl groups marked circled

cule was isolated from the sample data, was employed. To predict the activity of the separated molecules, the model acquired from the residual dataset was employed. PLS was analyzed through cross-validation to determine the optimum number of components (ONC). The final non-cross-validated CoMSIA and CoMFA models were developed using the ONC. The number of components that led to the highest coefficient of the cross-validated correlation (r_{cv}^2 or q^2) was considered as the ONC. To enhance efficiency and minimize noise, the employed column filtering was set to 2 kcal/mol. The optimum models were acquired by using the non-cross-validated analyses together with ONC, which provided the correlation coefficient r^2. To estimate predictive abilities, a test set of seven molecules that were excluded from the training set and aligned to the template was used. The coefficient of the predictive correlation (r_{pred}^2) was calculated by using an equation provided in the literature [18,19]. For a reliable model, r_{pred}^2 should be greater than 0.5 [20].

Docking study: The protein-ligand interactions were studied by selecting the molecule 29 as a reference molecule and it was docked into the active site of the HIV-1 RT (pdb code 3HVT) [21] with the aid of Surflex-Dock module of Tripos Inc. [17]. The X-ray crystal structures of HIV-1 RT (pdb code 3HVT) were collected from the Brookhaven Protein Data Bank (http://www.rcsb.org/pdb). An empirically scoring function was used in Surflex-Dock module [22,23]. For docking the ligands into the active site of the receptor, a licensed search engine was also used in the module. In the docking experiment, protein structure without energy minimization was utilized. By removing all the ligands and water molecules present in the receptor protein, polar hydrogen atoms were added. Protomol, an idealized charaterization of a ligand which is responsible for potential interaction with the receptor, was used to steer the molecular docking. Protomol is generated by 'automatic' option in Surflex-Dock that finds the biggest cavity in the receptor protein. The scoring function was tuned to estimate the binding affinities and the Surflex-Dock scores were expressed in the units of $-\log_{10}(K_d)^2$. The full scoring function is the sum of hydrophobic complementarity, repulsive complementarity, entropic and solvation terms. The various individual scoring functions was also combined to set up a consensus scoring function which is more robust in computing the interactions between ligand and receptor. Consensus score (CScore) [24] usually adds up different number of scoring functions to rank of binding affinity of the ligands, which are bound to the receptor's active site. The expected protein-ligand binding mode was visualized by using the Molecular Computer Aided Design (MOLCAD) program which was implemented in SYBYL-X [16].

RESULTS AND DISCUSSION

The best optimal CoMFA model employing steric and electrostatic fields was acquired with the ONC of 5 and cross-validated correlation coefficient (q^2) of 0.762. The non-cross-validated PLS analysis indicated a high correlation coefficient (r^2), good F value and low standard error estimate (S) of 0.952, 396 and 0.038, respectively. The contributions of steric and electrostatic and steric fields were found to be 0.640 and 0.360, respectively. Fig. 2 illustrates the correlation between the actual activities and the predicted activities of the training set and test sets.

In the CoMSIA model, various combinations of five CoMSIA fields were used to investigate the significance and predictivity. The optimal model was acquired using the hydrogen bond donor and electrostatic fields, which provided a q^2 and high non-cross-validated r^2 values of 0.758, and 0.957, respectively, with a low S and F values of 0.063 and 236, respectively. In this model, the hydrogen bond donor and electrostatic fields are found to contribute 0.657 and 0.343, respectively of the total field. Fig. 2 shows the relationship between the actual and the predicted pIC_{50} values both for the test and training sets for the CoMSIA model.

The external validations of CoMFA (r_{pred}^2 = 0.723) and CoMSIA (r_{pred}^2 = 0.693) models revealed a reliable and high predictive capacity of the new molecules.

Interpretation of 3D contour maps: Fig. 3a and Fig. 3b show the contour maps of the CoMFA steric and electrostatic fields, respectively, obtained from the final optimum non-cross-validated analysis. These maps revealed the zones in 3D space

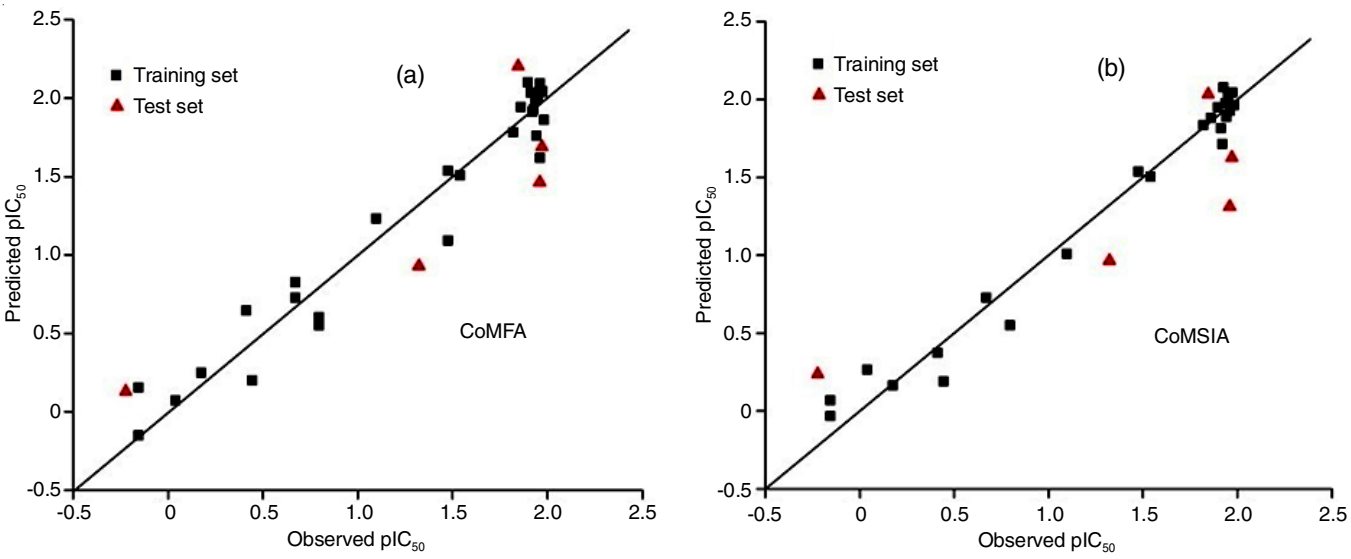

Fig. 2. Graph of actual *versus* predicted pIC_{50} of the training set and the test set using (a) CoMFA model and (b) CoMSIA model

available in the peripheral region of the aligned molecules, where changes in the steric and electrostatic fields would favour or disfavour the activity. For steric field, the CoMFA contour maps are shown by green and yellow contours. In the green and yellow regions, bulky and less bulky groups, respectively, are favourable, and the activity would decreases. It is evident from Fig. 3a that the prominent yellow contours are situated around the substituents R_1, R_2, R_3 and R_7, which indicated that non-bulky substituents are preferred at these positions.

On the other hand, blue contours around the substituent R_3, R_1 and R_8 are noticed due to the contribution of CoMFA electrostatic fields (Fig. 3a). At the same time, red contours are observed around the substituents R_1 and R_5. The blue contours implies more positive charge around R_3, R_1 and R_8 whereas the red contours around R_1 and R_5 indicate more negative charge which will increase the bio-activity. The blue contours are observed to be crowded over pyrone ring in the CoMSIA electrostatic map (Fig. 3c), which suggests the presence of more positive charge will increase the activity. The red contours are found to be located near R_1 which imply concentration of negative charge at this position will escalate the activity. In the CoMSIA hydrogen bond donor field (Fig. 3d), very distinct purple contours near R_1, R_2, R_3, R_7 and R_8 are observed which signifies that the hydrogen bond donor functionalities such as –OH or $–NH_2$ in these areas would boost the activity. This is in agreement with very high contribution (64.3%) of hydrogen bond donor. These observations are in fair agreement with experimental activity data of the set of molecules chosen. Molecule 14 (Morin) is most active having –OH donor group at R_1, R_2, R_3, R_5 and R_7 positions whereas molecule 1 (Kempferol) is second highest active having –OH donor groups at R_1, R_2, R_3 and R_7 positions.

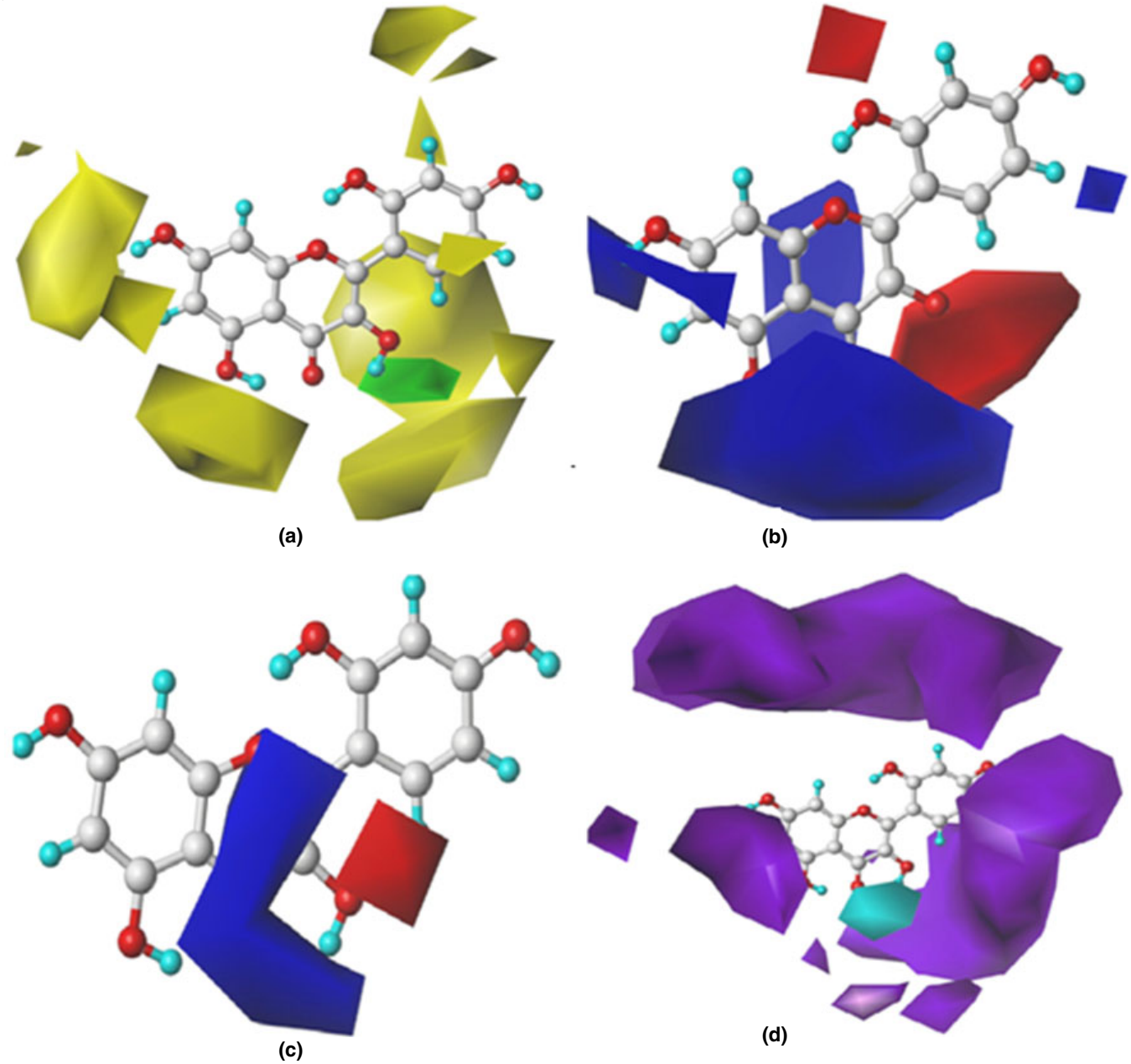

Fig. 3. (a) CoMFA contour maps for steric field, (b) CoMFA contour maps for electrostatic field, (c) CoMSIA contour maps for electrostatic field and (d) CoMSIA contour maps for hydrogen bond donor field, with highly active molecule 29, respectively

Docking study: Few flavonoids having the highest, intermediary, and lowest activities against AMV-RT were identified. These flavonoids were docked with HIV-RT. The most active AMV-RT inhibitor, compound 29, was docked to HIV-1 RT. The 40-OH, 5-OH, and 6-OH of scutellarein formed hydrogen bonds with the NH and carbonyl groups of Ile180; OH of Tyr319 and carbonyl group of His235; and NH of His235, respectively (Fig. 4). The binding interactions between HIV-RT and scutellarein were correlated with the flavonoid SAR as an AMV-RT inhibitor. For AMV-RT inhibition, two to three hydroxyl groups must be present in the vicinity of an aromatic ring. Compounds 20-29, containing 6-OH, provide effective inhibition against AMV-RT (>90% inhibition) and exhibit powerful binding to HIV 1-RT.

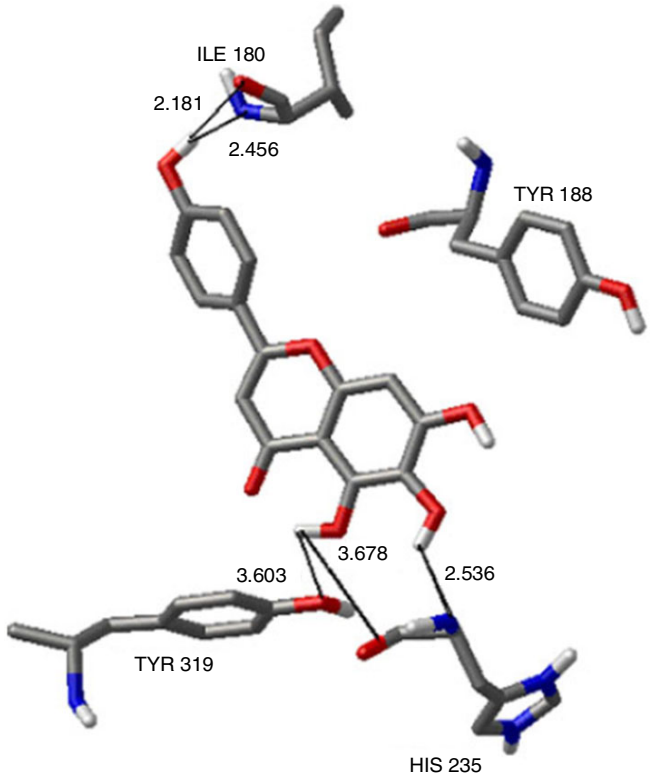

Fig. 4. Hydrogen bond interaction of flavonoid 29 with HIV-RT(3HVT) protein

For the inhibition activity, the substituents of hydrogen bonding are more responsible than other (electrostatic, steric, or hydrophobic) substituents. The findings of docking study indicated that the highly active AMV-RT inhibitors of flavonoid series having 6-OH structures can serve as potential HIV-1 RT inhibitors.

Conclusion

Reliable 3D-QSAR models implementing CoMFA and CoMSIA methods have been built for a set of 29 flavonoids. Molecules 1 and 14 have the maximum number of hydrogen bond donor positions exhibit higher activities. This is consistent with the results found with the CoMSIA method. It, therefore, can be posited principally that superior hydrogen bond donor groups at positions R_1, R_2, R_3, R_5 and R_7 is desired for superior radical scavenging activity of flavonoids. It is predictable both from the CoMFA and CoMSIA that electron withdrawing groups at position R_1 is preferable for higher radical scavenging activity. The present way of analysis by 3D-QSAR of the set of flavonoids selected will play an important role for finding out of better antioxidants. The docking analysis reveals the insight that hydrogen bonding and CH···π interaction happens in this type of molecules for docking with the HIV-RT protein (3HVT).

REFERENCES

1. D. Baltimore, Viral RNA-Dependent DNA Polymerase: RNA-Dependent DNA Polymerase in Virions of RNA Tumour Viruses, *Nature*, **226**, 1209 (1970); https://doi.org/10.1038/2261209a0
2. F. Barre-Sinoussi, J.C. Chermann, F. Rey, M.T. Nugeyre, S. Chamaret, J. Gruest, C. Dauguet, C. Axler-Blin, F. Vezinet-Brun, C. Rouzioux, W. Rozenbaum and L. Montagnier, Isolation of a T-lymphotropic Retrovirus from a Patient at Risk for Acquired Immune Deficiency Syndrome (AIDS), *Science*, **220**, 868 (1983); https://doi.org/10.1126/science.6189183
3. D.S. Auld, H. Kawaguchi, D.M. Livingston and B.L. Vallee, RNA-Dependent DNA Polymerase (Reverse Transcriptase) from Avian Myeloblastosis Virus: A Zinc Metalloenzyme, *Proc. Natl. Acad. Sci. USA*, **71**, 2091 (1974); https://doi.org/10.1073/pnas.71.5.2091
4. C.K. Tan, J. Zhang, Z.Y. Li, W.G. Tarpley, K.M. Downey and A.G. So, Functional Characterization of RNA-Dependent DNA Polymerase and RNase H Activities of a Recombinant HIV Reverse Transcriptase, *Biochemistry*, **30**, 2651 (1991); https://doi.org/10.1021/bi00224a013
5. T. Pengsuparp, L. Cai, H. Constant, H.H.S. Fong, L.Z. Lin, A.D. Kinghorn, J.M. Pezzuto, G.A. Cordell, K. Ingolfsdöttir, H. Wagner and S.H. Hughes, Mechanistic Evaluation of New Plant-Derived Compounds that Inhibit HIV-1 Reverse Transcriptase, *J. Nat. Prod.*, **58**, 1024 (1995); https://doi.org/10.1021/np50121a006
6. B. Havsteen, Flavonoids, A Class of Natural Products of High Pharmacological Potency, *Biochem. Pharmacol.*, **32**, 1141 (1983); https://doi.org/10.1016/0006-2952(83)90262-9
7. J.B. Harborne and C.A. Williams, Advances in Flavonoid Research Since 1992, *Phytochemistry*, **55**, 481 (2000); https://doi.org/10.1016/S0031-9422(00)00235-1
8. C.Q. Hu, K. Chen, Q. Shi, R.E. Kilkuskie, Y.C. Cheng and K.-H. Lee, Anti-AIDS Agents, 10. Acacetin-7-O-β-D-galactopyranoside, an Anti-HIV Principle from Chrysanthemum morifolium and a Structure-Activity Correlation with Some Related Flavonoids, *J. Nat. Prod.*, **57**, 42 (1994); https://doi.org/10.1021/np50103a006
9. M. Gabor, Anti-Inflammatory and Anti-Allergic Properties of Flavonoids, *Prog. Clin. Biol. Res.*, **213**, 471 (1986).
10. G. Spedding, A. Ratty and E. Middleton Jr., Inhibition of Reverse Transcriptases by Flavonoids, *Antiviral Res.*, **12**, 99 (1989); https://doi.org/10.1016/0166-3542(89)90073-9
11. I.T. Kusumoto, M. Hattori, Y. Miyaichi, T. Tomimori, M. Hanaoka and T. Namba, Effect of Flavonoids and Alkaloids on Reverse Transcriptase, *Shoyakugaku Zasshi*, **45**, 240 (1991).
12. R.D. Cramer, D.E. Patterson and J.D. Bunce, Comparative Molecular Field Analysis (CoMFA). 1. Effect of Shape on Binding of Steroids to Carrier Proteins, *J. Am. Chem. Soc.*, **110**, 5959 (1988); https://doi.org/10.1021/ja00226a005
13. S. Srivastava, W.W. Richardson, M.P. Bradley and G.M. Crippen, eds.: H. Kubinyi, Three-Dimensional Receptor Modeling using Distance Geometry and *Voronoi polyhedra*. In: 3D QSAR in Drug Design, Theory, Methods and Applications, ESCOM, Leiden, p. 409 (1993).
14. G. Klebe, U. Abraham and T. Mietzner, Molecular Similarity Indices in a Comparative Analysis (CoMSIA) of Drug Molecules to Correlate and Predict Their Biological Activity, *J. Med. Chem.*, **37**, 4130 (1994); https://doi.org/10.1021/jm00050a010
15. M. Bohm, J. Sturzebecher and G. Klebe, Three-Dimensional Quantitative Structure-Activity Relationship Analyses Using Comparative Molecular Field Analysis and Comparative Molecular Similarity Indices Analysis To Elucidate Selectivity Differences of Inhibitors Binding to Trypsin, Thrombin, and Factor Xa, *J. Med. Chem.*, **42**, 458 (1999); https://doi.org/10.1021/jm981062r

16. SYBYL-X 2.0, Tripos Inc, St. Louis (2013).
17. M.D.M. Abdul Hameed, A. Hamza, J. Liu and C.G. Zhan, Combined 3D-QSAR Modeling and Molecular Docking Study on Indolinone Derivatives as Inhibitors of 3-Phosphoinositide-Dependent Protein Kinase-1, *J. Chem. Inf. Model.*, **48**, 1760 (2008); https://doi.org/10.1021/ci800147v
18. D.M. Hawkins, S.C. Basak and D. Mills, Assessing Model Fit by Cross-Validation, *J. Chem. Inf. Comput. Sci.*, **43**, 579 (2003); https://doi.org/10.1021/ci025626i
19. A. Sarkar and A.D. Jana, Molecular Modeling of 4',5-Disubstituted Biphenyl Acetic Acid Molecules for their Anti-inflammatory Activity through 3D-QSAR, Docking and Molecular Dynamics Simulation, *Asian J. Chem.*, **30**, 2437 (2018); https://doi.org/10.14233/ajchem.2018.21434
20. A. Sarkar, T.R. Middya and A.D. Jana, A QSAR Study of Radical Scavenging Antioxidant Activity of a Series of Flavonoids using Dft Based Quantum Chemical Descriptors-The Importance of Group Frontier Electron Density, *J. Mol. Model.*, **18**, 2621 (2012); https://doi.org/10.1007/s00894-011-1274-2
21. S.J. Smerdon, J. Jäger, J. Wang, L.A. Kohlstaedt, A.J. Chirino, J.M. Friedman, P.A. Rice and T.A. Steitz, Structure of the Binding Site for Nonnucleoside Inhibitors of the Reverse Transcriptase of Human Immunodeficiency Virus Type 1, *Proc. Natl. Acad. Sci. (USA)*, **91**, 3911 (1994); https://doi.org/10.1073/pnas.91.9.3911
22. A.N. Jain, Surflex: Fully Automatic Flexible Molecular Docking Using a Molecular Similarity-Based Search Engine, *J. Med. Chem.*, **46**, 499 (2003); https://doi.org/10.1021/jm020406h
23. W. Welch, J. Rupper and A.N. Jain, Hammerhead: Fast, Fully Automated Docking of Flexible Ligands to Protein Binding Sites, *Chem. Biol.*, 3, 449 (1996); https://doi.org/10.1016/s1074-5521(96)90093-9
24. P.M. Marsden, D. Puvanendrampillai, J.B.O. Mitchell and R.C. Glen, Predicting Protein-Ligand Binding Affinities: A Low Scoring Game? *Org. Biomol. Chem.*, **2**, 3267 (2004); https://doi.org/10.1039/b409570g